Available online at www.sciencedirect.com
SCIENCE DIRECT®
Journal of Sound and Vibration 266 (2003) 737–757
JOURNAL OF SOUND AND VIBRATION
www.elsevier.com/locate/jsvi

A new exact substructure method using mixed modes

Ji-Bao Qiu[a], F.W. Williams[b,*], Ren-Xi Qiu[c]

[a] *Beijing Institute of Structure & Environment Engineering, Beijing 100076, People's Republic of China*
[b] *Department of Building and Construction, City University of Hong Kong, Kowloon, Hong Kong, People's Republic of China*
[c] *Cardiff University, Newport Road, Cardiff CF24 OYF, UK*

Received 4 June 2001; accepted 18 September 2002

Abstract

In this paper, the use of free- or fixed-interface modes in exact substructure displacement expansions is briefly summarized. Then the substructural displacements are expressed exactly in terms of mixed modes, i.e., the displacements consist of linear combinations of fixed- and free-interface modes. This yields a new exact mixed-mode substructure method. It is demonstrated that the exact substructure methods with fixed or free interfaces are two limiting cases of this new mixed-mode exact method. Thus, the exact substructure method variants with free-interface, fixed-interface or mixed modes form a systematic theory of substructure methods, which is unified by the new mixed-mode variant. This new exact variant not only has this important theoretical significance but also has great practical significance because it can lead to new approximate methods and to a deeper understanding of existing ones, e.g., quasi-comparison function methods, dynamic condensation methods or substructure modal synthesis methods.

1. Introduction

The substructure modal synthesis (SMS) method is one type of substructure method and is a modelling technique, which permits a complex structure to be represented by a reduced number of d.o.f. through modal transformation. SMS techniques are well known and popular in structural dynamic analysis and are very useful when solving large complex structural dynamic problems, especially for structures consisting of several obviously distinct substructures. They have been used widely in the aerospace and automotive industries and involve the structure as an assembly

*Corresponding author. Tel.: +852 21942045; fax: +852 27887612.
E-mail address: bcfred@cityu.edu.hk (F.W. Williams).

0022-460X/03/$ - see front matter © 2002 Elsevier Ltd. All rights reserved.
doi:10.1016/S0022-460X(02)01320-2

of substructures, which are then assembled together by satisfying compatibility and equilibrium at their interfaces.

Since Hurty presented his paper [1] on SMS in 1965, numerous variants of the SMS method have been presented. The Rayleigh–Ritz procedure permits them all to be described easily, but there are different substructure displacement representations, which need to be introduced by means of different mechanics analysis processes.

Due to the lack of a systematic framework, the variants of the SMS method were developed individually. The framework needed to unify them is now presented in this paper.

Compared to SMS, the exact substructure method (ESM) is another class of substructure methods, in which the number of d.o.f. of the structure is not reduced, thus giving the entire exact modes of the whole structure, i.e., the modes which would be obtained by using a direct analytical method.

There are three different forms of exact substructure displacement expansion expressions, namely the free-interface modes form, the fixed-interface modes form first presented in Ref [2], and the mixed modes form proposed in this paper. Hence, there are three different forms of dynamical analytical methods based on these.

A review of ESM with either free or fixed interfaces is presented in Sections 2.1 and 2.2. It is shown that the variants of SMS with either free or fixed interfaces are essentially different approximations to the ESM with free or fixed interfaces. This relationship between the variants of ESM and SMS gives new insights into the substructure method and is necessary for the systematization of such substructure methods. Hence, if new ESM variants can be constructed, related new SMS variants could be set up in terms of both the substructural displacement approximations and the synthesis procedures.

Using this approach, a new ESM variant using mixed modes is constructed in Section 3. By analytical means, the exact displacements are expressed exactly, as mixed modes consisting of linear combinations of the fixed- and free-interface modes. The exact results for the original whole structure, which would be obtained by using a direct analytical method, can instead be obtained exactly by using the new ESM proposed. This is proved by strict analytical derivation and demonstrated by numerical examples. It is also demonstrated that ESM with fixed or free interfaces are two limiting cases of this new ESM variant. Thus, the ESM variants using free, fixed or mixed modes form a systematic theory of substructure methods.

As already stated, the new mixed-mode ESM variant has great practical as well as theoretical significance. Hence, it is shown to have the capacity to lead to some new approximate methods or to a better understanding of existing ones, e.g., the assumed modes method using quasi-comparison functions [3,4], new dynamic condensation and new SMS variants. One of these, which was published recently [5], approximates the new ESM presented here by ignoring higher order mixed modes.

2. Three exact displacement expansion expressions

The equation of motion of each undamped substructure is

$$\boldsymbol{m}\ddot{\boldsymbol{X}} + \boldsymbol{k}\boldsymbol{X} = \boldsymbol{f} \tag{1}$$

where $\boldsymbol{m}$, $\boldsymbol{k}$, $\boldsymbol{X}$ and $\boldsymbol{f}$ are, respectively, the mass and stiffness matrices and the displacement and force vectors. This equation can be partitioned into

$$\begin{bmatrix} \boldsymbol{m}_{\mathrm{ii}} & \boldsymbol{m}_{\mathrm{ij}} \\ \boldsymbol{m}_{\mathrm{ji}} & \boldsymbol{m}_{\mathrm{jj}} \end{bmatrix} \begin{bmatrix} \ddot{\boldsymbol{X}}_{\mathrm{i}} \\ \ddot{\boldsymbol{X}}_{\mathrm{j}} \end{bmatrix} + \begin{bmatrix} \boldsymbol{k}_{\mathrm{ii}} & \boldsymbol{k}_{\mathrm{ij}} \\ \boldsymbol{k}_{\mathrm{ji}} & \boldsymbol{k}_{\mathrm{jj}} \end{bmatrix} \begin{bmatrix} \boldsymbol{X}_{\mathrm{i}} \\ \boldsymbol{X}_{\mathrm{j}} \end{bmatrix} = \begin{bmatrix} \boldsymbol{0} \\ \boldsymbol{f}_{\mathrm{j}} \end{bmatrix}, \tag{2}$$

where the subscripts i and j indicate internal and boundary d.o.f., respectively, and $\boldsymbol{f}_i = \boldsymbol{0}$, i.e. the forces corresponding to interior d.o.f., are all zero for the eigenvalue problem.

2.1. Exact displacement expansion expression using free-interface modes

The free vibration equation of any substructure with its interface free is Eq. (1) with $\boldsymbol{f} = \boldsymbol{0}$. The corresponding eigenvalue matrix $\boldsymbol{\Lambda}_E$, normal mode matrix $\boldsymbol{\Phi}_E$ and the relationships of orthonormality satisfy the equations

$$\boldsymbol{\Phi}_E^{\mathrm{T}} \boldsymbol{m} \boldsymbol{\Phi}_E = \boldsymbol{I}, \quad \boldsymbol{\Phi}_E^{\mathrm{T}} \boldsymbol{k} \boldsymbol{\Phi}_E = \boldsymbol{\Lambda}_E \tag{3}$$

in which

$$\begin{gathered} \boldsymbol{\Lambda}_E = \begin{bmatrix} \boldsymbol{0} & & \\ & \boldsymbol{\Lambda}_{El} & \\ & & \boldsymbol{\Lambda}_{Eh} \end{bmatrix}, \boldsymbol{\Phi}_E = [\boldsymbol{\Phi}_{ER}\ \boldsymbol{\Phi}_{EI}\ \boldsymbol{\Phi}_{Eh}], \\ \boldsymbol{\Lambda}_{El} = \left[\lambda_{E1}^2, \lambda_{E2}^2, \ldots, \lambda_{EL}^2\right], \quad \boldsymbol{\Lambda}_{Eh} = \left[\lambda_{E(L+1)}^2, \lambda_{E(L+2)}^2, \cdots, \lambda_{E(L+H)}^2\right], \end{gathered} \tag{4}$$

where subscript E indicates elements associated with free-interface substructures, $\boldsymbol{\Phi}_{ER}$ is the matrix of rigid-body modes, $\boldsymbol{\Lambda}_{El}$ is the diagonal matrix which comprises the L lowest non-zero eigenvalues λ, the diagonal matrix $\boldsymbol{\Lambda}_{Eh}$ comprises the remaining H (higher) eigenvalues λ and $\boldsymbol{\Phi}_{El}$ and $\boldsymbol{\Phi}_{Eh}$ contain the modes corresponding to $\boldsymbol{\Lambda}_{El}$ and $\boldsymbol{\Lambda}_{Eh}$.

From Eq. (1), the exact representation of modal co-ordinates for the substructure displacements $\boldsymbol{X}$ can be obtained analytically as

$$\begin{aligned} \boldsymbol{X} &= (\boldsymbol{k} - \boldsymbol{m}\omega^2)^{-1} \boldsymbol{f} = \boldsymbol{\Phi}_E (\boldsymbol{\Lambda}_E - \omega^2 \boldsymbol{I}_E) \boldsymbol{\Phi}_E^{\mathrm{T}} \boldsymbol{f} \\ &= \boldsymbol{X}_{ER} + \boldsymbol{X}_{El} + \boldsymbol{X}_{Eh} = \boldsymbol{\Phi}_{ER}\, \boldsymbol{q}_{ER} + \boldsymbol{\Phi}_{El} \boldsymbol{q}_{El} + \boldsymbol{\Phi}_{Eh} \boldsymbol{q}_{Eh} = \boldsymbol{\Phi}_E \bar{\boldsymbol{q}}_E, \end{aligned} \tag{5}$$

where

$$\begin{gathered} \boldsymbol{q}_{ER} = -\omega^{-2} \boldsymbol{\Phi}_{ER}^{\mathrm{T}} \boldsymbol{f}, \quad \boldsymbol{q}_{El} = (\boldsymbol{\Lambda}_{El} - \omega^2 \boldsymbol{I}_{El})^{-1} \boldsymbol{\Phi}_{El}^{\mathrm{T}} \boldsymbol{f}, \\ \boldsymbol{q}_{Eh} = (\boldsymbol{\Lambda}_{Eh} - \omega^2 \boldsymbol{I}_{Eh})^{-1} \boldsymbol{\Phi}_{Eh}^{\mathrm{T}} \boldsymbol{f}, \quad \boldsymbol{X}_{ER} = \boldsymbol{\Phi}_{ER} \boldsymbol{q}_{ER}, \quad \boldsymbol{X}_{El} = \boldsymbol{\Phi}_{El} \boldsymbol{q}_{El}, \\ \boldsymbol{X}_{Eh} = \boldsymbol{\Phi}_{Eh} \boldsymbol{q}_{Eh}, \quad \boldsymbol{\Phi}_E = \begin{bmatrix} \boldsymbol{\Phi}_{ER} & \boldsymbol{\Phi}_{El} & \boldsymbol{\Phi}_{Eh} \end{bmatrix}, \\ \bar{\boldsymbol{q}}_E = \begin{bmatrix} \boldsymbol{q}_{ER}^{\mathrm{T}} & \boldsymbol{q}_{El}^{\mathrm{T}} & \boldsymbol{q}_{Eh}^{\mathrm{T}} \end{bmatrix}^{\mathrm{T}}. \end{gathered} \tag{6}$$

According to classical modal theory, the complete set $\boldsymbol{\Phi}_E$ of free-interface modes is the complete set of substructure displacements and constitutes the complete space, while Eq. (5) represents the modes expansion theorem and $\bar{\boldsymbol{q}}_E$ are the modal co-ordinates.

Applying Eq. (5) to substructures enables the synthesis equation of exact free-interface substructure methods to be derived. Thus, the publications of Hou [6], MacNeal [7], Ruben [8], Craig and Chang [9], Wang et al. [10], Qiu and Tan [11] and Ying et al. [12] construct a systematic logical progression of SMS variants, which essentially are different approximations to the ESM variant which uses free-interface modes. Thus, this ESM formulation is the theoretical basis of all practical approximate SMS variant methods which use free interfaces.

2.2. Exact displacement expansion expression using fixed-interface modes

For a fixed interface denoted by j, the displacement vector is

$$\boldsymbol{X}_b = \begin{Bmatrix} \boldsymbol{X}_{bi} \\ \boldsymbol{X}_{bj} \end{Bmatrix} = \begin{Bmatrix} \boldsymbol{X}_{bi} \\ \boldsymbol{0} \end{Bmatrix} \tag{7}$$

and so Eq. (2) simplifies to

$$\boldsymbol{m}_{ii}\ddot{\boldsymbol{X}}_{bi} + \boldsymbol{k}_{ii}\boldsymbol{X}_{bi} = \boldsymbol{0}, \quad \boldsymbol{m}_{ji}\ddot{\boldsymbol{X}}_{bi} + \boldsymbol{k}_{ji}\boldsymbol{X}_{bi} = \boldsymbol{f}_{bj}, \tag{8}$$

where the subscript b indicates that the element is associated with a fixed-interface substructure and $\boldsymbol{f}_{bj}$ is the force vector at the fixed interface. The corresponding eigenvalue matrix $\boldsymbol{\Lambda}_b$, normal mode matrix $\boldsymbol{\Phi}_b$ and relationships of orthonormality satisfy the equations

$$\boldsymbol{\Phi}_b^{\mathrm{T}}\boldsymbol{k}\boldsymbol{\Phi}_b = \boldsymbol{\Phi}_{bi}^{\mathrm{T}}\boldsymbol{k}_{ii}\boldsymbol{\Phi}_{bi} = \boldsymbol{\Lambda}_b, \quad \boldsymbol{\Phi}_b^{\mathrm{T}}\boldsymbol{m}\boldsymbol{\Phi}_b = \boldsymbol{\Phi}_{bi}^{\mathrm{T}}\boldsymbol{m}_{ii}\boldsymbol{\Phi}_{bi} = \boldsymbol{I}_b \tag{9}$$

in which, with $\lceil \ldots \rfloor$ denoting a diagonal matrix,

$$\boldsymbol{\Lambda}_b = \begin{bmatrix} \boldsymbol{\Lambda}_{bl} & \boldsymbol{0} \\ \boldsymbol{0} & \boldsymbol{\Lambda}_{bh} \end{bmatrix} \quad \boldsymbol{\Phi}_b = \begin{bmatrix} \boldsymbol{\Phi}_{bi} \\ \boldsymbol{0} \end{bmatrix} = \begin{bmatrix} \boldsymbol{\Phi}_{bl} & \boldsymbol{\Phi}_{bh} \end{bmatrix},$$

$$\boldsymbol{\Lambda}_{bl}\left\lceil \lambda_{b1}^2, \lambda_{b2}^2, \ldots \lambda_{bL}^2 \right\rfloor; \boldsymbol{\Lambda}_{bh} = \left\lceil \lambda_{b(L+1)}^2, \lambda_{b(L+2)}^2, \ldots, \lambda_{b(L+H)}^2 \right\rfloor, \tag{10}$$

where the diagonal matrices $\boldsymbol{\Lambda}_{bl}$ and $\boldsymbol{\Lambda}_{bh}$ involve, respectively, the L lowest eigenvalues and the remaining H (higher) eigenvalues and $\boldsymbol{\Phi}_{bl}$ and $\boldsymbol{\Phi}_{bh}$ contain the corresponding modes.

The next step is to use an analytical method to obtain an exact expression for the substructural displacements, as follows. If the interfaces had not been fixed, the first row of Eq. (2) would give

$$(\boldsymbol{k}_{ii} - \omega^2\boldsymbol{m}_{ii})\boldsymbol{X}_i + (\boldsymbol{k}_{ij} - \omega^2\boldsymbol{m}_{ij})\boldsymbol{X}_j = \boldsymbol{0}. \tag{11}$$

Therefore, the displacements $\boldsymbol{X}_i$ at the internal d.o.f. i and X can be expressed exactly in terms of the boundary displacements $\boldsymbol{X}_j$ as

$$\begin{gathered} \boldsymbol{X}_i = \boldsymbol{t}_{ci}\boldsymbol{X}_j, \quad \boldsymbol{X} = \begin{bmatrix} \boldsymbol{X}_i \\ \boldsymbol{X}_j \end{bmatrix} = \boldsymbol{T}_c\boldsymbol{X}_j, \\ \boldsymbol{T}_c = \begin{bmatrix} \boldsymbol{t}_{ci} \\ \boldsymbol{I} \end{bmatrix}, \quad \boldsymbol{t}_{ci} = -\bar{\boldsymbol{R}}(\omega^2)(\boldsymbol{k}_{ij} - \omega^2\boldsymbol{m}_{ij}), \end{gathered} \tag{12}$$

$$\bar{\boldsymbol{R}}(\omega^2) = (\boldsymbol{k}_{ii} - \omega^2\boldsymbol{m}_{ii})^{-1} = (\boldsymbol{k}_{ii} - \omega^2\boldsymbol{m}_{ii})^{-1}(\boldsymbol{k}_{ii} - \omega^2\boldsymbol{m}_{ii} + \omega^2\boldsymbol{m}_{ii})\boldsymbol{k}_{ii}^{-1}$$
$$= [I + \omega^2(\boldsymbol{k}_{ii} - \omega^2\boldsymbol{m}_{ii})^{-1}\boldsymbol{m}_{ii}]\boldsymbol{k}_{ii}^{-1} = \boldsymbol{k}_{ii}^{-1} + \omega^2\bar{\boldsymbol{R}}(\omega^2)\boldsymbol{m}_{ii}\boldsymbol{k}_{ii}^{-1}. \tag{13}$$

Here $\boldsymbol{T}_c$ and $\bar{\boldsymbol{R}}(\omega^2)$ are the exact constraint mode and dynamic flexibility matrix of the constrained substructure. Substituting Eq. (13) into Eq. (12) and using Eq. (9) gives exact constraint modes, for use with the complete set of fixed-interface normal modes as follows

$$\boldsymbol{t}_{ci} = -\boldsymbol{k}_{ii}^{-1}\boldsymbol{k}_{ij} + \omega^2\boldsymbol{\Phi}_{bi}(\boldsymbol{\Lambda}_b - \omega^2\boldsymbol{I}_b)^{-1}\boldsymbol{\Phi}_b^{\mathrm{T}}\boldsymbol{m}\boldsymbol{\Phi}_{c0}, \tag{14}$$

$$\boldsymbol{T}_c = \boldsymbol{\Phi}_{c0} + \omega^2\boldsymbol{\Phi}_b(\boldsymbol{\Lambda}_b - \omega^2\boldsymbol{I}_b^{\mathrm{T}})^{-1}\boldsymbol{\Phi}_b^{\mathrm{T}}\boldsymbol{m}\boldsymbol{\Phi}_{c0}, \tag{15a}$$

$$\boldsymbol{\Phi}_{c0} = \begin{bmatrix} \boldsymbol{t}_{c0} \\ \boldsymbol{I} \end{bmatrix}, \tag{15b}$$

$$\boldsymbol{t}_{c0} = -\boldsymbol{k}_{ii}^{-1}\boldsymbol{k}_{ij}. \tag{15c}$$

Substituting Eq. (15a) into Eq. (12) gives the exact displacements $\boldsymbol{X}$ in terms of the complete set of fixed-interface normal modes as

$$\boldsymbol{X} = \boldsymbol{X}_{c0} + \boldsymbol{X}_{bl} + \boldsymbol{X}_{bh} = \boldsymbol{\Phi}_B\bar{\boldsymbol{q}}_B, \tag{16}$$

where

$$\boldsymbol{X}_{c0} = \boldsymbol{\Phi}_{c0}\boldsymbol{X}_j, \quad \boldsymbol{X}_{bl} = \boldsymbol{\Phi}_{bl}\boldsymbol{q}_{bl}, \quad \boldsymbol{X}_{bh} = \boldsymbol{\Phi}_{bh}\boldsymbol{q}_{bh},$$
$$\boldsymbol{\Phi}_B = \begin{bmatrix} \boldsymbol{\Phi}_{c0} & \boldsymbol{\Phi}_{bl} & \boldsymbol{\Phi}_{bh} \end{bmatrix}, \quad \bar{q}_B = \begin{bmatrix} \boldsymbol{X}_j^{\mathrm{T}} & \boldsymbol{q}_{bl}^{\mathrm{T}} & \boldsymbol{q}_{bh}^{\mathrm{T}} \end{bmatrix}^{\mathrm{T}}, \tag{17}$$
$$\boldsymbol{q}_{bl} = \omega^2(\boldsymbol{\Lambda}_b - \omega^2\boldsymbol{I}_b)\boldsymbol{\Phi}_{bl}^T\boldsymbol{m}\boldsymbol{\Phi}_{c0}\boldsymbol{X}_j, \quad \boldsymbol{q}_{bh} = \omega^2(\boldsymbol{\Lambda}_b - \omega^2\boldsymbol{I}_b)\boldsymbol{\Phi}_{bh}^{\mathrm{T}}\boldsymbol{m}\boldsymbol{\Phi}_{c0}\boldsymbol{X}_j,$$

Eq. (16) means that the static constraint modes $\boldsymbol{\Phi}_{c0}$, plus the complete set $\boldsymbol{\Phi}_b$ of fixed-interface normal modes, form the complete set of substructure displacements $\boldsymbol{X}$ and $\bar{\boldsymbol{q}}_B$ are modal co-ordinates, so that the space constituted is complete, as was also true for the alternative exact expansion expression of Section 2.1.

Applying Eq. (16) to substructures enables the synthesis equation of fixed-interface ESMs to be derived. Thus, the publications of Hurty [1], Craig and Bampton [13] and Qiu et al. [2] build a systematic logical progression of methods, which essentially involve different approximations to the ESM variant which uses fixed-interface modes. Hence, the fixed-interface variant of ESM is important because it is the theoretical basis of all practical approximate fixed-interface modal synthesis methods.

2.3. Relationships between rigid-body modes and static constraint modes

From Eq. (15), $\boldsymbol{\Phi}_{c0}$ is the modal matrix associated with the so-called static constraint modes, while $\boldsymbol{t}_{c0}$ is the static displacement matrix corresponding to the internal d.o.f., i, of which the lth column is the displacement vector due to $\boldsymbol{X}_j$ having a unit value as its lth element, with all its other elements assumed to be zero. Now the interface constrained force $\boldsymbol{f}_{c0j}$ can be expressed as

$$\boldsymbol{f}_{c0j} = \boldsymbol{k}_{jj} - \boldsymbol{k}_{ji}\boldsymbol{k}_{ii}^{-1}\boldsymbol{k}_{ij}, \tag{18}$$

so that

$$\boldsymbol{k}\boldsymbol{\Phi}_{c0} = \begin{bmatrix} \mathbf{0} \\ \boldsymbol{f}_{c0j} \end{bmatrix}. \tag{19}$$

For any substructure with fixed interfaces, the number of interface d.o.f., j, cannot be less than the number of rigid-body d.o.f., R, of the substructure with its interfaces free. There are statically determinate constrained modes $\boldsymbol{\Phi}_{cR}$ and redundant constrained modes $\boldsymbol{\Phi}_{cc}$. Let

$$\boldsymbol{\Phi}_{c0} = \begin{bmatrix} \boldsymbol{\Phi}_{cR} & \boldsymbol{\Phi}_{cc} \end{bmatrix}, \tag{20a}$$

$$\boldsymbol{f}_{c0j} = \begin{bmatrix} \boldsymbol{f}_{cRj} & \boldsymbol{f}_{ccj} \end{bmatrix}. \tag{20b}$$

The interface force $\boldsymbol{f}_{cRj}$ of the statically determinate constrained modes must satisfy the static equilibrium equations

$$\boldsymbol{f}_{cRj}\boldsymbol{L}_R = \mathbf{0}, \tag{21}$$

where there must exist an $R \times R$ matrix $\boldsymbol{L}_R$ and a $J \times R$ matrix $\boldsymbol{L}_J$,

$$\boldsymbol{L}_J = \begin{bmatrix} \boldsymbol{L}_R \\ \mathbf{0} \end{bmatrix}. \tag{22}$$

The $\boldsymbol{f}_{c0j}$ of the RHS of Eq. (19) must satisfy the equilibrium equations, which are also of order R. Hence, using Eqs. (20b)–(22) gives

$$\begin{bmatrix} \mathbf{0} \\ \boldsymbol{f}_{c0j} \end{bmatrix} \boldsymbol{L}_J = \begin{bmatrix} \mathbf{0} \\ \boldsymbol{f}_{c0j}\boldsymbol{L}_J \end{bmatrix} = \begin{bmatrix} \mathbf{0} \\ \boldsymbol{f}_{cRj}\boldsymbol{L}_R \end{bmatrix} = \mathbf{0}. \tag{23}$$

Substituting Eq. (19) into Eq. (23) gives

$$\boldsymbol{k}\boldsymbol{\Phi}_{c0}\boldsymbol{L}_J = \boldsymbol{k}\boldsymbol{\Phi}_{ER} = \begin{bmatrix} \mathbf{0} \\ \boldsymbol{f}_{\mathrm{c0j}} \end{bmatrix} \boldsymbol{L}_J = \mathbf{0}, \tag{24}$$

where, see Eqs. (20a), (22) and (24),

$$\boldsymbol{\Phi}_{ER} = \boldsymbol{\Phi}_{c0}\boldsymbol{L}_J = \begin{bmatrix} \boldsymbol{\Phi}_{cR} & \boldsymbol{\Phi}_{cc} \end{bmatrix} \begin{bmatrix} \boldsymbol{L}_R \\ \mathbf{0} \end{bmatrix} = \boldsymbol{\Phi}_{cR}\boldsymbol{L}_R \tag{25}$$

which shows that $\boldsymbol{\Phi}_{ER}$ must, by definition, be rigid-body modes. Hence, Eq. (25) shows that the rigid-body modes $\boldsymbol{\Phi}_{ER}$ can be represented as a linear combination of the statically determinate constrained modes.

From Eq. (25),

$$\boldsymbol{\Phi}_{cR} = \boldsymbol{\Phi}_{ER}\bar{\boldsymbol{q}}_{cR}, \tag{26a}$$

$$\bar{\boldsymbol{q}}_{cR} = \boldsymbol{L}_R^{\mathrm{T}}(\boldsymbol{L}_R\boldsymbol{L}_R^{\mathrm{T}})^{-1}. \tag{26b}$$

Substituting Eqs. (20a) and (26a) into Eq. (16) gives another form of the exact displacement $\boldsymbol{X}$ as

$$\boldsymbol{X} = \boldsymbol{\Phi}_{BE}\boldsymbol{q}_{BE}, \tag{27}$$

where

$$\boldsymbol{\Phi}_{BE} = \begin{bmatrix} \boldsymbol{\Phi}_{ER} & \boldsymbol{\Phi}_{cc} & \boldsymbol{\Phi}_{bl} & \boldsymbol{\Phi}_{bh} \end{bmatrix}, \quad \boldsymbol{q}_{BE} = \begin{bmatrix} \boldsymbol{q}_{ER}^{\mathrm{T}} & \boldsymbol{X}_{cj}^{\mathrm{T}} & \boldsymbol{q}_{bl}^{\mathrm{T}} & \boldsymbol{q}_{bh}^{\mathrm{T}} \end{bmatrix}^{\mathrm{T}},$$

$$\boldsymbol{X}_{c0} = \boldsymbol{\Phi}_{c0}\boldsymbol{X}_j = \begin{bmatrix} \boldsymbol{\Phi}_{cR} & \boldsymbol{\Phi}_{cc} \end{bmatrix} \begin{Bmatrix} \boldsymbol{X}_{Rj} \\ \boldsymbol{X}_{cj} \end{Bmatrix} = \begin{bmatrix} \boldsymbol{\Phi}_{ER} & \boldsymbol{\Phi}_{cc} \end{bmatrix} \begin{Bmatrix} \boldsymbol{q}_{ER} \\ \boldsymbol{X}_{cj} \end{Bmatrix}, \quad \boldsymbol{q}_{ER} = \bar{\boldsymbol{q}}_{cR}\boldsymbol{X}_{Rj}. \tag{28}$$

Eq. (27) is equivalent to the statement that the complete set of substructure displacements $\boldsymbol{X}$ is equivalent to the complete set $\boldsymbol{\Phi}_b$ of fixed-interface normal modes, plus rigid-body modes $\boldsymbol{\Phi}_{ER}$ and redundant constrained modes $\boldsymbol{\Phi}_{cc}$.

2.4. Exact displacement expansion expression using mixed substructure modes

Because it implies the modes expansion theorem, Eq. (5) can be used to represent any substructure displacements. Thus, the fixed-interface modes can be expressed exactly in terms of the free-interface modes as

$$\begin{bmatrix} \boldsymbol{\Phi}_{cc} & \boldsymbol{\Phi}_{bl} \end{bmatrix} = \boldsymbol{\Phi}_{ER}\boldsymbol{q}_{bER} + \boldsymbol{\Phi}_{El}\boldsymbol{q}_{bEl} + \boldsymbol{\Phi}_{Eh}\boldsymbol{q}_{bEh}. \tag{29}$$

For any substructure, the lower modes are usually obtained more easily than the higher ones, whether from test data or from numerical analysis. Therefore, it is easier to find the redundant constrained modes $\boldsymbol{\Phi}_{cc}$ and the lower fixed-interface modes $\boldsymbol{\Phi}_{bl}$ than to find the higher free-interface modes $\boldsymbol{\Phi}_{Eh}$. Let H_E be the number of higher free-interface modes $\boldsymbol{\Phi}_{Eh}$ for a substructure, while L_c is the total number of redundant constrained modes $\boldsymbol{\Phi}_{cc}$ and lower fixed interfacial modes $\boldsymbol{\Phi}_{bl}$ retained. If the number of higher modes is chosen so that $L_c = H_E$, to ensure that the total number of modes used equals the number of substructure d.o.f. ($=N$), Eq. (29) gives exactly

$$\boldsymbol{\Phi}_{Eh} = (\begin{bmatrix} \boldsymbol{\Phi}_{cc} & \boldsymbol{\Phi}_{bl} \end{bmatrix} - \boldsymbol{\Phi}_{ER}\boldsymbol{q}_{bER} - \boldsymbol{\Phi}_{El}\boldsymbol{q}_{bEl})\boldsymbol{q}_{ch} \tag{30a}$$

$$\boldsymbol{q}_{ch} = \boldsymbol{q}_{bEh}^{\mathrm{T}}(\boldsymbol{q}_{bEh}\boldsymbol{q}_{bEh}^{\mathrm{T}})^{-1} \tag{30b}$$

i.e., the higher free-interface modes have been expressed in terms of some lower mixed modes. Substituting Eq. (30a) into Eq. (5) gives Eq. (31) and then substituting Eqs. (20a) and (25) into Eq. (31) gives Eq. (32):

$$\begin{aligned} X &= \boldsymbol{\Phi}_{ER}\boldsymbol{q}_{ER} + \boldsymbol{\Phi}_{El}\boldsymbol{q}_{El} + (\begin{bmatrix} \boldsymbol{\Phi}_{cc} & \boldsymbol{\Phi}_{bl} \end{bmatrix} - \boldsymbol{\Phi}_{ER}\boldsymbol{q}_{bER} - \boldsymbol{\Phi}_{El}\boldsymbol{q}_{bEl})\boldsymbol{q}_{ch}\boldsymbol{q}_{Eh} \\ &= \boldsymbol{\Phi}_{ER}\boldsymbol{q}_R + \boldsymbol{\Phi}_{cc}\boldsymbol{q}_c + \boldsymbol{\Phi}_{bl}\boldsymbol{q}_b + \boldsymbol{\Phi}_{El}\boldsymbol{q}_E, \end{aligned} \tag{31}$$

$$\boldsymbol{X} = \boldsymbol{\Phi}_{c0}\boldsymbol{q}_{c0} + \boldsymbol{\Phi}_{El}\boldsymbol{q}_E + \boldsymbol{\Phi}_{bl}\boldsymbol{q}_b \tag{32}$$

where

$$\begin{aligned} &\boldsymbol{q}_{CE} = \boldsymbol{q}_{ch}\boldsymbol{q}_{Eh}, \quad \boldsymbol{q}_R = \boldsymbol{q}_{ER} - \boldsymbol{q}_{bER}\boldsymbol{q}_{CE}, \quad \boldsymbol{q}_E = \boldsymbol{q}_{El} - \boldsymbol{q}_{bEl}\boldsymbol{q}_{CE} \\ &\boldsymbol{q}_{CE} = \begin{bmatrix} \boldsymbol{q}_c \\ \boldsymbol{q}_b \end{bmatrix}, \quad \boldsymbol{q}_{c0} = \begin{bmatrix} \boldsymbol{L}_R\boldsymbol{q}_R \\ \boldsymbol{q}_c \end{bmatrix} \end{aligned} \tag{33}$$

Hence, the substructural displacement $\boldsymbol{X}$ has been expressed exactly in terms of lower mixed modes, i.e. as a linear combination of the static constraint modes $\boldsymbol{\Phi}_{c0}$, the lower free-interface

modes $\boldsymbol{\Phi}_{El}$ and the lower fixed-interface modes $\boldsymbol{\Phi}_{bl}$. This is a third possible exact expansion expression, in addition to those of Sections 2.1 and 2.2.

If $R \neq 0$ and $j = R$, i.e., the number of rigid-body d.o.f. equals the number of interfacial d.o.f., then the redundant constrained modes $\boldsymbol{\Phi}_{cc}$ vanish. Hence Eq. (31) simplifies to

$$\boldsymbol{X} = \boldsymbol{\Phi}_{ER}\boldsymbol{q}_R + \boldsymbol{\Phi}_{El}\boldsymbol{q}_E + \boldsymbol{\Phi}_{bl}\boldsymbol{q}_b \tag{34}$$

3. New ESM mixed-mode variant

3.1. Substructure dynamic equation for mixed-modes ESM

Eq. (32) can be written as

$$\boldsymbol{X} = \boldsymbol{\Phi}\boldsymbol{q} \tag{35a}$$

$$\boldsymbol{\Phi} = \begin{bmatrix} \boldsymbol{\Phi}_{c0} & \boldsymbol{\Phi}_{El} & \boldsymbol{\Phi}_{bl} \end{bmatrix}, \tag{35b}$$

$$\boldsymbol{q} = \begin{bmatrix} \boldsymbol{q}_{c0}^{\mathrm{T}} & \boldsymbol{q}_E^{\mathrm{T}} & \boldsymbol{q}_b^{\mathrm{T}} \end{bmatrix}^{\mathrm{T}}, \tag{35c}$$

Then substituting Eq. (35a) into Eq. (1) and pre-multiplying by $\boldsymbol{\Phi}^{\mathrm{T}}$ leads to the exact substructure dynamic equation of the new method

$$(\boldsymbol{k}_n - \omega^2 \boldsymbol{m}_n)\boldsymbol{q} = \boldsymbol{f}_n, \tag{36}$$

where

$$\boldsymbol{k}_n = \begin{bmatrix} \boldsymbol{k}_0 & \boldsymbol{k}_{0E} & \boldsymbol{0} \\ \boldsymbol{k}_{E0} & \boldsymbol{\Lambda}_{El} & \boldsymbol{k}_{Eb} \\ \boldsymbol{0} & \boldsymbol{k}_{bE} & \boldsymbol{\Lambda}_{bl} \end{bmatrix}, \quad \boldsymbol{m}_n = \begin{bmatrix} \boldsymbol{m}_0 & \boldsymbol{m}_{0E} & \boldsymbol{m}_{0b} \\ \boldsymbol{m}_{E0} & \boldsymbol{I}_{El} & \boldsymbol{m}_{Eb} \\ \boldsymbol{m}_{b0} & \boldsymbol{m}_{bE} & \boldsymbol{I}_{bl} \end{bmatrix}, \quad \boldsymbol{f}_n = \begin{bmatrix} \boldsymbol{I}_{c0}\boldsymbol{f}_j \\ \boldsymbol{\Phi}_{Elj}^{\mathrm{T}}\boldsymbol{f}_j \\ \boldsymbol{0} \end{bmatrix},$$

$$\begin{aligned} \boldsymbol{k}_0 &= \boldsymbol{\Phi}_{c0}^{\mathrm{T}}\boldsymbol{k}\boldsymbol{\Phi}_{c0}, \quad \boldsymbol{k}_{Eb} = \boldsymbol{k}_{bE}^{\mathrm{T}} = \boldsymbol{\Phi}_{El}^{\mathrm{T}}\boldsymbol{k}\boldsymbol{\Phi}_{bl}, \quad \boldsymbol{k}_{E0} = \boldsymbol{k}_{0E}^{T} = \boldsymbol{\Phi}_{c0}^{T}\boldsymbol{k}\boldsymbol{\Phi}_{El}, \\ \boldsymbol{m}_0 &= \boldsymbol{\Phi}_{c0}^{T}\boldsymbol{m}\boldsymbol{\Phi}_{c0}, \quad \boldsymbol{m}_{0E} = \boldsymbol{m}_{E0}^{\mathrm{T}} = \boldsymbol{\Phi}_{c0}^{\mathrm{T}}\boldsymbol{m}\boldsymbol{\Phi}_{El}, \\ \boldsymbol{m}_{Eb} &= \boldsymbol{m}_{bE}^{\mathrm{T}} = \boldsymbol{\Phi}_{El}^{\mathrm{T}}\boldsymbol{m}\boldsymbol{\Phi}_{bl}, \quad \boldsymbol{m}_{0b} = \boldsymbol{m}_{b0}^{\mathrm{T}} = \boldsymbol{\Phi}_{c0}^{\mathrm{T}}\boldsymbol{m}\boldsymbol{\Phi}_{bl}. \end{aligned} \tag{37}$$

3.2. Whole structure dynamic equation for mixed-mode ESM

For simplicity, attention is restricted to cases with only adjacent substructures α and β, but the extension to more general cases is not difficult. Using Eq. (36) for both substructures gives

$$\left(\begin{bmatrix} \boldsymbol{k}_{n\alpha} & \boldsymbol{0} \\ \boldsymbol{0} & \boldsymbol{k}_{n\beta} \end{bmatrix} - \omega^2 \begin{bmatrix} \boldsymbol{m}_{n\alpha} & \boldsymbol{0} \\ \boldsymbol{0} & \boldsymbol{m}_{n\beta} \end{bmatrix} \right) \begin{bmatrix} \boldsymbol{q}_\alpha \\ \boldsymbol{q}_\beta \end{bmatrix} = \begin{bmatrix} \boldsymbol{f}_{n\alpha} \\ \boldsymbol{f}_{n\beta} \end{bmatrix}. \tag{38}$$

From Eq. (35) and the interface compatibility relationship $\boldsymbol{X}_{j\alpha} = \boldsymbol{X}_{j\beta}$,

$$\boldsymbol{q}_{c0\alpha} = \boldsymbol{N}_1\boldsymbol{Q}, \ \boldsymbol{Q} = \begin{bmatrix} \boldsymbol{q}_{E\alpha}^{\mathrm{T}} & \boldsymbol{q}_{b\alpha}^{\mathrm{T}} & \boldsymbol{q}_{c0\beta}^{\mathrm{T}} & \boldsymbol{q}_{E\beta}^{\mathrm{T}} & \boldsymbol{q}_{b\beta}^{\mathrm{T}} \end{bmatrix}^{\mathrm{T}} \tag{39}$$

so that

$$\boldsymbol{q}_{\alpha\beta} = \boldsymbol{N}\boldsymbol{Q}, \tag{40}$$

where

$$\boldsymbol{N}_1 = \begin{bmatrix} -\boldsymbol{\Phi}_{Elj\alpha} & \boldsymbol{0} & \boldsymbol{I}_{j\beta} & \boldsymbol{\Phi}_{Elj\beta} & \boldsymbol{0} \end{bmatrix},$$

$$\boldsymbol{q}_{\alpha\beta} = \begin{bmatrix} \boldsymbol{q}_\alpha^{\mathrm{T}} & \boldsymbol{q}_\beta^{\mathrm{T}} \end{bmatrix}^{\mathrm{T}}, \quad \boldsymbol{N} = \begin{bmatrix} \boldsymbol{N}_1 \\ \boldsymbol{I} \end{bmatrix}. \tag{41}$$

Substituting the transformation of Eq. (40), pre-multiplying by $\boldsymbol{N}^{\mathrm{T}}$, and using the interface equilibrium equation, $\boldsymbol{f}_{j\alpha} + \boldsymbol{f}_{j\beta} = \boldsymbol{0}$, transforms Eq. (38) into the exact whole structure dynamic equation of the new exact mixed-mode variant of ESM, i.e.,

$$(\boldsymbol{K} - \omega^2 \boldsymbol{M})\boldsymbol{Q} = \boldsymbol{0}, \tag{42}$$

where

$$\boldsymbol{K} = \boldsymbol{N}^{\mathrm{T}} \begin{bmatrix} \boldsymbol{k}_{n\alpha} & \boldsymbol{0} \\ \boldsymbol{0} & \boldsymbol{k}_{n\beta} \end{bmatrix} \boldsymbol{N}, \quad \boldsymbol{M} = \boldsymbol{N}^{\mathrm{T}} \begin{bmatrix} \boldsymbol{m}_{n\alpha} & \boldsymbol{0} \\ \boldsymbol{0} & \boldsymbol{m}_{n\beta} \end{bmatrix} \boldsymbol{N}. \tag{43}$$

Eq. (42) is a linear dynamic equation for the whole structure and includes completely the contribution of all the higher modes. So this new ESM variant not only gives exact results but also has a simple form with linear synthesis equations.

3.3. Case of statically determinate interface for mixed-mode ESM

If the number of interface d.o.f., j, equals the number of rigid-body d.o.f., R, the substructural displacements have been shown to be given in terms of the mixed modes $\boldsymbol{\Phi}_{El}, \boldsymbol{\Phi}_{ER}$ and $\boldsymbol{\Phi}_{bl}$ by Eq. (34), i.e., by

$$\boldsymbol{X} = \bar{\boldsymbol{\Phi}}\bar{\boldsymbol{q}}, \tag{44a}$$

$$\bar{\boldsymbol{\Phi}} = \begin{bmatrix} \boldsymbol{\Phi}_{ER} & \boldsymbol{\Phi}_{El} & \boldsymbol{\Phi}_{bl} \end{bmatrix}, \tag{44b}$$

$$\bar{\boldsymbol{q}} = \begin{bmatrix} \boldsymbol{q}_R^{\mathrm{T}} & \boldsymbol{q}_E^{\mathrm{T}} & \boldsymbol{q}_b^{\mathrm{T}} \end{bmatrix}^{\mathrm{T}}. \tag{44c}$$

Substituting Eq. (44a) into Eq. (1) and pre-multiplying by $\bar{\boldsymbol{\Phi}}^{\mathrm{T}}$ leads to the exact substructure dynamic equation

$$(\bar{\boldsymbol{k}}_n - \omega^2 \bar{\boldsymbol{m}}_n)\bar{\boldsymbol{q}} = \bar{\boldsymbol{f}}_n. \tag{45}$$

Here, proceeding exactly analogously to the derivations of Eqs. (36)–(43), the exact whole structure dynamic equation is

$$(\bar{\boldsymbol{K}} - \omega^2 \bar{\boldsymbol{M}})\bar{\boldsymbol{Q}} = \boldsymbol{0}, \quad \bar{\boldsymbol{Q}} = \begin{bmatrix} \boldsymbol{q}_{E\alpha}^{\mathrm{T}} & \boldsymbol{q}_{b\alpha}^{\mathrm{T}} & \boldsymbol{q}_{R\beta}^{\mathrm{T}} & \boldsymbol{q}_{E\beta}^{\mathrm{T}} & \boldsymbol{q}_{b\beta}^{\mathrm{T}} \end{bmatrix}^{\mathrm{T}} \tag{46}$$

and by using Eqs. (3), (9) and (24),

$$\bar{\boldsymbol{k}}_n = \begin{bmatrix} \boldsymbol{0} & \boldsymbol{0} \\ \boldsymbol{0} & \boldsymbol{K}_{Eb} \end{bmatrix}, \quad \boldsymbol{K}_{Eb} = \begin{bmatrix} \boldsymbol{\Lambda}_{El} & \bar{\boldsymbol{k}}_{Eb} \\ \bar{\boldsymbol{k}}_{bE} & \boldsymbol{\Lambda}_{bl} \end{bmatrix},$$

$$\bar{\boldsymbol{m}}_n = \begin{bmatrix} \boldsymbol{I}_R & \bar{\boldsymbol{m}}_{RE} & \bar{\boldsymbol{m}}_{Rb} \\ \bar{\boldsymbol{m}}_{ER} & \boldsymbol{I}_{El} & \bar{\boldsymbol{m}}_{Eb} \\ \bar{\boldsymbol{m}}_{bR} & \bar{\boldsymbol{m}}_{bE} & \boldsymbol{I}_{bl} \end{bmatrix}, \quad \bar{\boldsymbol{f}}_n = \begin{bmatrix} \boldsymbol{\Phi}_{ERj}^{\mathrm{T}} \boldsymbol{f}_j \\ \boldsymbol{\Phi}_{Elj}^{\mathrm{T}} \boldsymbol{f}_j \\ \boldsymbol{0} \end{bmatrix},$$

$$\bar{\boldsymbol{k}}_{Eb} = \bar{\boldsymbol{k}}_{bE}^{\mathrm{T}} = \boldsymbol{\Phi}_{El}^{\mathrm{T}} \boldsymbol{k} \boldsymbol{\Phi}_{bl}, \quad \bar{\boldsymbol{m}}_{RE} = \bar{\boldsymbol{m}}_{ER}^{\mathrm{T}} = \boldsymbol{\Phi}_{ER}^{\mathrm{T}} \boldsymbol{m} \boldsymbol{\Phi}_{El},$$

$$\bar{\boldsymbol{m}}_{Rb} = \bar{\boldsymbol{m}}_{bR}^{\mathrm{T}} = \boldsymbol{\Phi}_{ER}^{\mathrm{T}} \boldsymbol{m} \boldsymbol{\Phi}_{bl}, \quad \bar{\boldsymbol{m}}_{Eb} = \bar{\boldsymbol{m}}_{bE}^{\mathrm{T}} = \boldsymbol{\Phi}_{El}^{\mathrm{T}} \boldsymbol{m} \boldsymbol{\Phi}_{bl},$$

$$\bar{\boldsymbol{K}} = \bar{\boldsymbol{N}}^{\mathrm{T}} \begin{bmatrix} \bar{\boldsymbol{k}}_{n\alpha} & \boldsymbol{0} \\ \boldsymbol{0} & \bar{\boldsymbol{k}}_{n\beta} \end{bmatrix} \bar{\boldsymbol{N}} = \begin{bmatrix} \boldsymbol{K}_{Ec\alpha} & \boldsymbol{0} & \boldsymbol{0} \\ \boldsymbol{0} & \boldsymbol{0} & \boldsymbol{0} \\ \boldsymbol{0} & \boldsymbol{0} & \boldsymbol{K}_{Ec\beta} \end{bmatrix}, \quad \bar{\boldsymbol{M}} = \bar{\boldsymbol{N}}^{\mathrm{T}} \begin{bmatrix} \bar{\boldsymbol{m}}_{n\alpha} & \boldsymbol{0} \\ \boldsymbol{0} & \bar{\boldsymbol{m}}_{n\beta} \end{bmatrix} \bar{\boldsymbol{N}},$$

$$\bar{\boldsymbol{N}}_1 = \boldsymbol{\Phi}_{ERj\alpha}^{-1} \begin{bmatrix} -\boldsymbol{\Phi}_{Elj\alpha} & \boldsymbol{0} & \boldsymbol{\Phi}_{ERj\beta} & \boldsymbol{\Phi}_{Elj\beta} & \boldsymbol{0} \end{bmatrix}, \quad \bar{\boldsymbol{N}} = \begin{bmatrix} \bar{\boldsymbol{N}}_1 \\ \boldsymbol{I} \end{bmatrix},$$

$$\bar{\boldsymbol{q}}_{\alpha\beta} = \begin{bmatrix} \boldsymbol{q}_{R\alpha}^{\mathrm{T}} & \boldsymbol{q}_{E\alpha}^{\mathrm{T}} & \boldsymbol{q}_{b\alpha}^{\mathrm{T}} & \boldsymbol{q}_{R\beta}^{\mathrm{T}} & \boldsymbol{q}_{E\beta}^{\mathrm{T}} & \boldsymbol{q}_{b\beta}^{\mathrm{T}} \end{bmatrix}^{\mathrm{T}}, \quad \bar{\boldsymbol{q}}_{\alpha\beta} = \overline{\boldsymbol{N}\boldsymbol{Q}}. \tag{47}$$

4. Numerical example for new mixed-mode ESM

4.1. Example 1

Consider axial vibration of the mathematical model of the whole bar shown in Fig. 1(a). This uniform free–free bar can be divided into two substructures, each of which is further divided into two identical bar elements, see Fig. 1(b) and (c). Hence, $N=3$ and the stiffness and mass matrices of each bar element are

$$\boldsymbol{K} = k \begin{bmatrix} 1 & -1 \\ -1 & 1 \end{bmatrix}, \quad \boldsymbol{M} = m \begin{bmatrix} 1 & 0 \\ 0 & 1 \end{bmatrix}. \tag{48a}$$

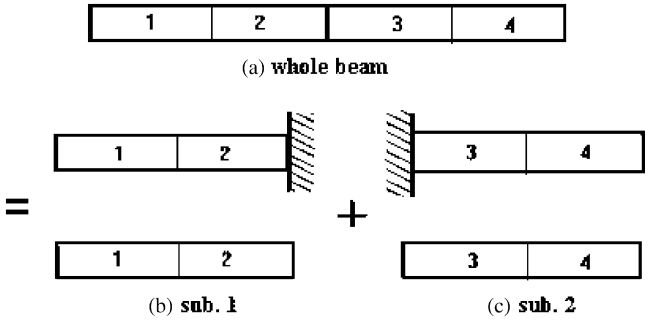

Fig. 1. Free–free bar with two substructures of equal length.

In order to enable the accuracy of the proposed exact method to be checked, the exact eigenvalues and eigenvectors of the whole mathematical model of the bar were obtained as

$$\omega^2 = 0, \frac{2-\sqrt{2}}{2}\frac{k}{m}, \frac{k}{m}, \frac{2+\sqrt{2}}{2}\frac{k}{m}, 2\frac{k}{m}, \tag{48b}$$

$$\boldsymbol{\Phi} = \frac{1}{2\sqrt{2m}}\begin{bmatrix} 1 & \sqrt{2} & \sqrt{2} & -\sqrt{2} & 1 \\ 1 & 1 & 0 & 1 & -1 \\ 1 & 0 & -\sqrt{2} & 0 & 1 \\ 1 & -1 & 0 & -1 & -1 \\ 1 & -\sqrt{2} & \sqrt{2} & \sqrt{2} & 1 \end{bmatrix}. \tag{48c}$$

These solutions are the datum results.

For substructure 1, the exact eigenvalues and modes with its interface fixed were obtained as

$$\omega^2 = \frac{2-\sqrt{2}}{2}\frac{k}{m}, \frac{2+\sqrt{2}}{2}\frac{k}{m} \tag{49a}$$

$$\boldsymbol{\Phi}_b = \begin{bmatrix} \boldsymbol{\Phi}_{bl} & \boldsymbol{\Phi}_{bh} \end{bmatrix} = \frac{1}{2\sqrt{m}}\begin{bmatrix} \sqrt{2} & \sqrt{2} \\ 1 & -1 \\ 0 & 0 \end{bmatrix} \tag{49b}$$

whereas with its interface free they were found to be

$$\omega^2 = 0, \frac{k}{m}, \frac{2k}{m}, \tag{50a}$$

$$\boldsymbol{\Phi}_E = \begin{bmatrix} \boldsymbol{\Phi}_{ER} & \boldsymbol{\Phi}_{El} & \boldsymbol{\Phi}_{Eh} \end{bmatrix} = \frac{1}{2\sqrt{m}}\begin{bmatrix} 1 & \sqrt{2} & 1 \\ 1 & 0 & -1 \\ 1 & -\sqrt{2} & 1 \end{bmatrix}. \tag{50b}$$

The displacement of substructure 1, i.e., $\boldsymbol{X}_1$, can be represented exactly in terms of the above two kinds of modes, i.e., the mixed modes $\bar{\boldsymbol{\Phi}}_1$, as

$$\boldsymbol{X}_1 = \bar{\boldsymbol{\Phi}}_1 \bar{\boldsymbol{q}}_1 \tag{51}$$

for which the interface displacement $\boldsymbol{X}_{1j}$ is

$$\boldsymbol{X}_{1j} = \frac{1}{2\sqrt{m}}(-\sqrt{2}\boldsymbol{q}_{E1} + \boldsymbol{q}_{R1}), \tag{52}$$

where the mixed modes $\bar{\boldsymbol{\Phi}}_1$ consist of two kinds of lower modes of substructure 1, being the rigid-body mode $\boldsymbol{\Phi}_{ER}$ and the lowest mode $\boldsymbol{\Phi}_{El}$ with free interface, see Eq. (50b), and the lowest mode $\boldsymbol{\Phi}_{bl}$ with interface fixed, see Eq. (49b), so that the number of modes used is equal to number

of d.o.f. N (=3) and

$$\bar{\boldsymbol{\Phi}}_1 = \begin{bmatrix} \boldsymbol{\Phi}_{ER} & \boldsymbol{\Phi}_{El} & \boldsymbol{\Phi}_{bl} \end{bmatrix} = \frac{1}{2\sqrt{m}} \begin{bmatrix} 1 & \sqrt{2} & \sqrt{2} \\ 1 & 0 & 1 \\ 1 & -\sqrt{2} & 0 \end{bmatrix}, \quad \bar{\boldsymbol{q}}_1 = \begin{bmatrix} \bar{\boldsymbol{q}}_R & \bar{\boldsymbol{q}}_E & \bar{\boldsymbol{q}}_b \end{bmatrix}^{\mathrm{T}}. \tag{53}$$

From Eq. (36), the vibration equation corresponding to the displacement $\boldsymbol{X}_1$ of substructure 1 is

$$(\bar{\boldsymbol{k}}_1 - \omega^2 \bar{\boldsymbol{m}}_1)\bar{\boldsymbol{q}}_1 = \bar{\boldsymbol{f}}_1, \quad \bar{\boldsymbol{f}} = \begin{bmatrix} \boldsymbol{0} \\ \boldsymbol{f}_{1j} \end{bmatrix}, \tag{54}$$

where the generalized stiffness, mass and force matrices are given, using Eqs. (37) and (53), by

$$\bar{\boldsymbol{k}}_1 = \bar{\boldsymbol{\Phi}}_1^{\mathrm{T}} \boldsymbol{k}_1 \bar{\boldsymbol{\Phi}}_1, \quad \bar{\boldsymbol{m}}_1 = \bar{\boldsymbol{\Phi}}_1^{\mathrm{T}} \boldsymbol{m}_1 \bar{\boldsymbol{\Phi}}_1, \quad \bar{\boldsymbol{f}}_1 = \bar{\boldsymbol{\Phi}}_1^{\mathrm{T}} \boldsymbol{f}. \tag{55}$$

Similarly, for substructure 2, the vibration equation is

$$(\bar{\boldsymbol{k}}_2 - \omega^2 \bar{\boldsymbol{m}}_2)\bar{\boldsymbol{q}}_2 = \bar{\boldsymbol{f}}_2, \quad \boldsymbol{X}_{2j} = \frac{1}{2\sqrt{m}}(-\sqrt{2}\boldsymbol{q}_{E2} + \boldsymbol{q}_{R2}),$$

$$\bar{\boldsymbol{k}}_2 = \bar{\boldsymbol{k}}_1, \quad \bar{\boldsymbol{m}}_2 = \bar{\boldsymbol{m}}_1, \tag{56a}$$

$$\bar{f}_2 = \begin{bmatrix} \boldsymbol{0} \\ \boldsymbol{f}_{2j} \end{bmatrix}_2. \tag{56b}$$

Combining Eqs. (38), (54) and (56a) gives the vibration equation for the mathematical model of the whole bar as

$$\left(\bar{\boldsymbol{K}}_{12} - \omega^2 \bar{\boldsymbol{M}}_{12}\right)\bar{\boldsymbol{q}}_{12} = \bar{\boldsymbol{F}}_{12}, \tag{57}$$

where, see Eqs. (38) and (41),

$$\overline{\boldsymbol{K}}_{12} = \begin{bmatrix} \bar{\boldsymbol{k}}_1 & \boldsymbol{0} \\ \boldsymbol{0} & \bar{\boldsymbol{k}}_2 \end{bmatrix}, \quad \bar{\boldsymbol{M}}_{12} = \begin{bmatrix} \bar{\boldsymbol{m}}_1 & \boldsymbol{0} \\ \boldsymbol{0} & \bar{\boldsymbol{m}}_2 \end{bmatrix}, \quad \bar{\boldsymbol{F}}_{12} = \begin{bmatrix} \bar{\boldsymbol{f}}_1 \\ \bar{\boldsymbol{f}}_2 \end{bmatrix},$$

$$\overline{\boldsymbol{q}}_{12} = \begin{bmatrix} \boldsymbol{q}_{R1}^{\mathrm{T}} & \boldsymbol{q}_{E1}^{\mathrm{T}} & \boldsymbol{q}_{b1}^{\mathrm{T}} & \boldsymbol{q}_{R2}^{\mathrm{T}} & \boldsymbol{q}_{E2}^{\mathrm{T}} & \boldsymbol{q}_{b2}^{\mathrm{T}} \end{bmatrix}^{\mathrm{T}}. \tag{58}$$

The compatibility and equilibrium relationships between the interface displacements and interface forces of substructures 1 and 2 are

$$\boldsymbol{X}_{1j} = \boldsymbol{X}_{2j}, \tag{59a}$$

$$\boldsymbol{f}_{1j} + \boldsymbol{f}_{2j} = \boldsymbol{0}. \tag{59b}$$

Eqs. (52), (56b) and (59a) give

$$\boldsymbol{q}_{R1} = \sqrt{2}\boldsymbol{q}_{E1} + \boldsymbol{q}_{R2} - \sqrt{2}\boldsymbol{q}_{E2} \tag{60}$$

and so Eqs. (39)–(41) give the transformation as

$$\bar{\boldsymbol{q}}_{12} = \bar{\boldsymbol{N}}_{12}\bar{\boldsymbol{Q}}, \tag{61a}$$

$$\bar{\boldsymbol{N}}_{12} = \begin{bmatrix} \sqrt{2} & 0 & 1 & -\sqrt{2} & 0 \\ 1 & 0 & 0 & 0 & 0 \\ 0 & 1 & 0 & 0 & 0 \\ 0 & 0 & 1 & 0 & 0 \\ 0 & 0 & 0 & 1 & 0 \\ 0 & 0 & 0 & 0 & 1 \end{bmatrix}, \tag{61b}$$

$$\bar{\boldsymbol{Q}} = \begin{bmatrix} \boldsymbol{q}_{E1} \\ \boldsymbol{q}_{b1} \\ \boldsymbol{q}_{R2} \\ \boldsymbol{q}_{E2} \\ \boldsymbol{q}_{b2} \end{bmatrix}. \tag{61c}$$

Substituting Eq. (61a) into Eq. (57) and pre-multiplying by $\bar{\boldsymbol{N}}_{12}^{\mathrm{T}}$ gives the exact vibration equation for the mathematical model of the whole bar as

$$(\bar{\boldsymbol{K}} - \omega^2\bar{\boldsymbol{M}})\bar{\boldsymbol{Q}} = \bar{\boldsymbol{F}} = \boldsymbol{0}, \tag{62}$$

where, from Eq. (43),

$$\bar{\boldsymbol{K}} = \bar{\boldsymbol{N}}_{12}^{\mathrm{T}}\bar{\boldsymbol{K}}_{12}\bar{\boldsymbol{N}}_{12}, \quad \bar{\boldsymbol{M}} = \bar{\boldsymbol{N}}_{12}^{\mathrm{T}}\bar{\boldsymbol{M}}_{12}\bar{\boldsymbol{N}}_{12}. \tag{63}$$

The eigenvalue equation is

$$\left|\bar{\boldsymbol{K}} - \omega^2\bar{\boldsymbol{M}}\right| = 0. \tag{64}$$

Substituting Eq. (63) into Eq. (64) and expanding gives

$$\omega^2\left(\omega^4 - 2\omega^2\frac{k}{m} + 0.5\frac{k^2}{m^2}\right)\left(\omega^2 - \frac{k}{m}\right)\left(\omega^2 - 2\frac{k}{m}\right) = 0 \tag{65}$$

which generates exactly the answers given in Eq. (48b), i.e., the exact eigenvalues for the mathematical model of the whole bar. Then substituting Eq. (48b) into Eq. (64) generates exactly the modes given in Eq. (48c), i.e., the exact eigenvectors for the mathematical model of the whole bar. This shows that the exact eigenvalues and eigenvectors can be obtained by using the new mixed-mode ESM variant.

4.2. Example 2

Consider axial vibration of the mathematical model of the whole bar shown in Fig. 2(a). This uniform free-free bar is divided into two unequal substructures, see Figs. 2(b) and (c), then substructure 1 is further divided into six identical bar elements, so that $N_1 = 7$, and substructure 2 is further divided into eight identical bar elements, giving $N_2 = 9$. Hence, the stiffness and mass

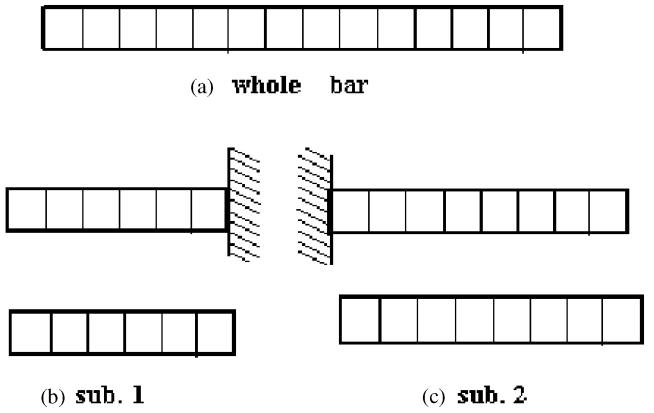

Fig. 2. Free–free bar with two substructures, with the length of substructure 1 being 0.75 × length of substructure 2.

matrices of the bar elements are

$$\boldsymbol{K} = 4k\begin{bmatrix} 1 & -1 \\ -1 & 1 \end{bmatrix}, \quad \boldsymbol{M} = 0.25m\begin{bmatrix} 1 & 0 \\ 0 & 1 \end{bmatrix}. \tag{66}$$

Because there were so many d.o.f. an analytical solution was not obtained. Instead a high accuracy eigenvalue calculation program was used to obtain the datum solution for this example and also for Examples 3 and 4 below. The results are shown in Table 1, for which exceptionally high accuracy was used throughout to give the very high accuracy of the table, including in the free- and fixed-interface mode calculations. Similar accuracy was also used in Examples 3 and 4. The ESM calculations used the same high accuracy program as was used to obtain the datum solution and this procedure was also used for Examples 3 and 4.

The N_1 (= 7) modes used by the ESM calculations for substructure 1 were: one rigid-body mode ($R_1 = 1$); the lowest L_{E1} free-interface modes, and the lowest L_{c1} free–fixed interface modes, with the left-hand end free. Similarly, the N_2(= 9) modes used by the ESM calculations for substructure 2 were: one rigid-body mode ($R_2 = 1$); the lowest L_{E2} free interface modes and; the lowest L_{c2} free-fixed interface modes, with the right-hand end free. Table 1 gives five different combinations of L_{E1}, L_{c1}, L_{E2} and L_{c2}, as cases A–E. Hence, it can be seen that the mixed-mode ESM has $L_{E1} + L_{c1} + R_1 = N_1$ for substructure 1 and $L_{E2} + L_{c2} + R_2 = N_2$ for substructure 2. The errors of the synthesis frequencies for cases A–E are listed in Table 1.

For case A, the lower fixed-interface modes $\boldsymbol{\Phi}_{bl}$ are absent, $L_{c1} = L_{c2} = 0$, $L_{E1} = 6$ and $L_{E2} = 8$ so that $L_E + R = N$, i.e., case A is the free-interface ESM case. Similarly, for case E the free-interface modes $\boldsymbol{\Phi}_{El}$ are absent, i.e., $L_{E1} = L_{E2} = 0$, $L_{c1} = 6$ and $L_{c2} = 8$, so that $L_c + R = N$, i.e., case E is the fixed-interface ESM case.

4.3. Example 3

Consider vibration of the mathematical model of the whole beam shown in Fig. 3(a). This uniform free–free beam, with $l = 0.5$ m, can be divided into two substructures of equal length

Table 1
Error (%) of synthesis frequencies ($\omega_i = 1, 2, \ldots, 15$) for the free–free bar of Fig. 2

		Free-interface ESM	Mixed–mode ESM			Fixed interface ESM	Datum $\omega(\times\sqrt{k/m})$
Case		A	B	C	D	E	
$N_1(=7)$	L_{E1}	6	5	3	1	0	
	L_{c1}	0	1	3	5	6	
$N_2(=9)$	L_{E2}	8	6	4	2	0	
	L_{c2}	0	2	4	6	8	
Error ($\times 100\%$)	1	—	—	—	—	—	0.33422138886441675409778143208 6e−15
	2	4.20e−31	5.10e–28	2.80e−25	3.40e–29	0.0	0.63336722437185112733758570679
	3	3.10e−31	7.90e−27	3.30e−25	1.80e–28	0.0	1.25876849085179041918058179613 0
	4	2.10e−31	3.10e−26	1.60e–23	8.30e–29	0.0	1.86834051513944402304133594663 6
	5	3.50e−31	1.30e−26	5.80e−24	3.70e−28	0.0	2.45441707341280192448154397821 7
	6	1.90e−31	1.10e−26	4.90e−24	1.30e−28	0.31e−30	3.00962791290203681091691647398 7
	7	1.20e−31	9.30e−26	4.60e−24	1.20e−28	0.26e−30	3.52699093515973890025776922670 2
	8	1.20e−14	6.50e−15	1.40e−11	3.00e−28	0.0	4.00000000000000000000000000000 0
	9	1.50e−31	5.50e−26	3.60e−23	1.90e−29	0.20e−30	4.42270674398620176800741670887 6
	10	2.10e−31	3.90e−25	3.00e−22	1.00e−27	0.84e−30	4.78979538455255204522813698996 6
	11	8.70e−32	6.40e−25	1.50e−20	1.10e−28	0.20e−30	5.09664956905413857868056487899 1
	12	5.50e−32	3.80e−24	6.10e−21	1.70e−27	0.73e−30	5.33941042807990898684748260941 9
	13	2.60e−31	2.40e−23	1.00e−19	4.70e−28	0.14e−29	5.51502510297448292764162473398 1
	14	1.00e−31	2.00e−23	1.70e−20	3.60e−27	0.14e−29	5.62128513730705335693379764272 2
	15	1.80e−31	4.20e−23	3.00e−20	4.20e−26	0.12e−29	5.65685424949238019520675489684 5

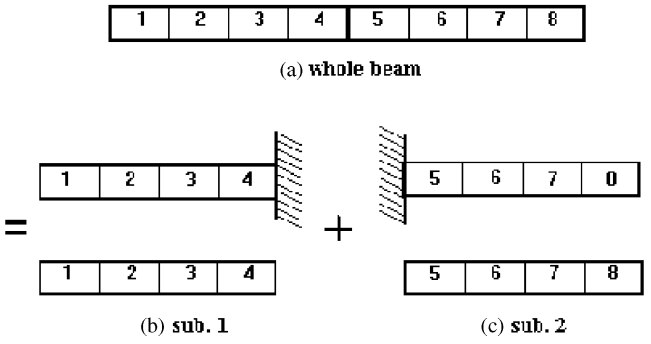

Fig. 3. Free–free beam with two substructures of equal length.

$l = 0.25$ m, each of which is further divided into four identical beam elements, see Figs. 3(b) and (c). Hence, $N = 10$ and the stiffness and mass matrices of the beam elements are

$$\boldsymbol{K} = \frac{EI}{l^3}\begin{bmatrix} 12 & 6l & -12 & 6l \\ 6l & 4l^2 & -6l & 2l^2 \\ -12 & -6l & 12 & 22l \\ 6l & 2l^2 & 22l & 4l^2 \end{bmatrix}, \quad \boldsymbol{M} = \frac{\rho Al}{420}\begin{bmatrix} 156 & 22l & 54 & -13l \\ 22l & 4l^2 & 13l & -3l^2 \\ 54 & 13l & 156 & -22l \\ -13l & -3l^2 & -22l & 4l^2 \end{bmatrix}, \tag{67}$$

where E is Young's modulus, ρ is mass density, I is cross-sectional second moment of area, A is area and $EI/\rho A = 0.1\ \mathrm{m}^4/\mathrm{s}^2$.

Two rigid-body modes, the lowest five free-interface modes and the lowest three free–fixed interface modes, were the $N(=10)$ modes used for each substructure, with the left-hand (right-hand) end free for substructure 1 (2). The results are given in Table 2 and again indicate that the mixed-mode ESM gave the exact results expected.

4.4. Example 4

Consider in-plane vibration of the mathematical model of the whole rectangular plate with free sides shown in Fig. 4(a), for which length $4a = 2$ m, width $2b = 1$ m and thickness $h = 0.02$ m. Young's modulus $E = 10.5 \times 10^9$ Pa, $\mu = 0.3$ and mass density $\rho = 1 \times 10^3\ \mathrm{kg/m}^3$. The plate was divided into the two substructures shown in Figs. 4(b) and (c), each of which was treated as a single square plate element. Hence $N = 8$ and the element stiffness and mass matrices were both (8×8) matrices. Further details of the stiffness and mass matrices are not given for reasons of space, nor are the results tabulated, because it is sufficient to record that the mixed-mode ESM gave the 12 natural frequencies to an accuracy of, at worst, 8.6×10^{-16} % when the $N(=8)$ modes used were three rigid-body ones, the lowest three free interface ones and the lowest two fixed interface ones.

Table 2
Synthesis frequencies ($f_i = 1, 2, \ldots, 18$) for free–free beam of Fig. 3 ($\omega = 2\pi f$)

i	Mixed–mode ESM		Datum
	f (Hz)	Error (%)	f (Hz)
1	0		0
2	0		0
3	45.50214540	1.97e−13	45.50214540
4	125.4914907	2.01e−13	125.4914907
5	246.3890073	5.05e−15	246.3890073
6	408.6039666	2.94e−14	408.6039666
7	613.6316784	3.34e−16	613.6316784
8	862.6159881	3.97e−14	862.6159881
9	1144.350291	3.82e−14	1144.350291
10	1603.172312	1.80e−13	1603.172312
11	2020.985894	4.57e−12	2020.985894
12	2547.696916	3.55e−15	2547.696916
13	3190.630241	8.96e−11	3190.630241
14	3973.896293	1.17e−11	3973.896293
15	4909.563874	3.52e−09	4909.563874
16	5922.807511	2.77e−10	5922.807511
17	7765.700339	5.02e−09	7765.700339
18	7818.807397	3.68e−10	7818.807397

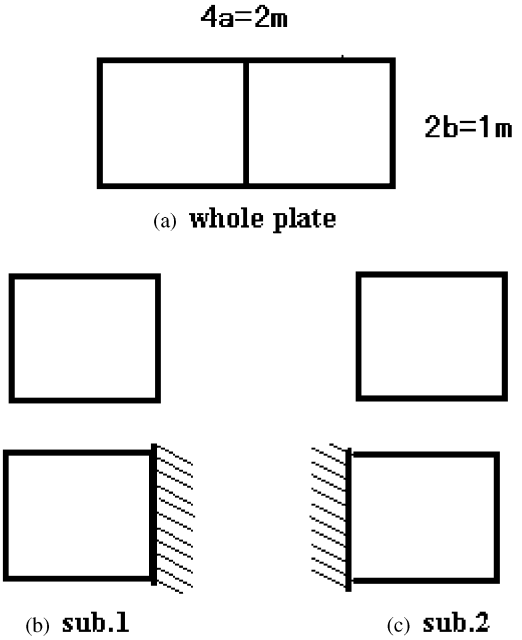

Fig. 4. Free plate with two substructures of equal length.

5. Discussion of the importance of the new mixed-mode ESM

5.1. Two limiting cases of the new mixed-mode ESM

R is the number of rigid-body modes, L_c is the number of redundant constrained modes $\boldsymbol{\Phi}_{cc}$ and lower fixed-interface modes $\boldsymbol{\Phi}_{bl}$, and L_E is the number of lower free-interface modes $\boldsymbol{\Phi}_{El}$ for a substructure with N d.o.f. Therefore, the mixed-mode ESM has $L_E + L_c + R = N$. When the redundant constrained modes $\boldsymbol{\Phi}_{cc}$ and the lower fixed-interface modes $\boldsymbol{\Phi}_{bl}$ are both absent, $L_c = 0$ and so $L_E + R = N$. Then Eqs. (31) and (42) reduce to the substructure displacement Eq. (5) and the whole structure dynamic equation of free-interface ESM. Alternatively, if the free-interface modes $\boldsymbol{\Phi}_{El}$ are absent, $L_E = 0$ and so $L_c + R = N$. Then Eqs. (32) and (42) reduce to the substructure displacement Eq. (16) and the whole structure dynamic equation of fixed interface ESM. Therefore, ESM using either free- or fixed-interface modes are limiting cases of the new mixed-mode ESM, which is thus a unifying theory for understanding and systematizing all ESM variants.

Obviously, all SMS variants are essentially different approximations to ESM. Hence, an important aspect of the new mixed-mode ESM is that it enables new approximate methods to be developed that also use mixed modes or approximations to them, e.g., see Qiu et al. [5] and the assumed modes method using quasi-comparison functions [3,4] briefly described in the next subsection.

5.2. Assumed modes method using quasi-comparison function

The new mixed-mode ESM includes two types of finite series of modes in the substructural displacement $\boldsymbol{X}$, see Eqs. (31) and (32). If these two types of mode are replaced by two types of admissible function, the result is the assumed modes method using quasi-comparison functions [3,4], as described further below.

Meirovitch and Kwak [3] demonstrated that the usually used form of the classical Rayleigh–Ritz method could have impaired convergence characteristics due to the following implicit flaw. If the eigenvalue problem is formulated as a variational problem, the Rayleigh–Ritz method consists of constructing a sequence of approximate solutions from the space of admissible functions. These admissible functions can be expressed in the form of a series of trial functions and the accuracy of the sequence of approximations is improved by increasing the number of terms in this series. The trial functions are commonly taken as members of the same family of functions, but unfortunately solutions thus obtained are often characterized by poor convergence. The cause is that natural boundary conditions are often very difficult to satisfy when using relatively few admissible functions. The fact that Rayleigh–Ritz theory guarantees convergence provided the admissible functions are from a complete set is small comfort in computational work, where good accuracy is required from as few terms as possible.

To overcome this predicament, Meirovitch and Kwak [3] proposed constructing the approximating sequence from the space of quasi-comparison functions, instead of merely from the space of admissible functions. Quasi-comparison functions are linear combinations of admissible functions that act like comparison functions. The aim is to select admissible functions, which are able to satisfy the natural boundary conditions. This involves using several different

types of admissible function. It is this variety of admissible functions that permits accurate satisfaction of the natural boundary conditions while using only relatively few terms.

Meirovitch and Kwak [4] state that the concept of quasi-comparison functions is particularly powerful in substructure synthesis using assumed modes, such that when they are used to approximate the motion of substructures the connection conditions between substructures can be satisfied to any required accuracy by only a finite number of terms. Hence, eigensolutions obtained by using quasi-comparison functions as the assumed modes exhibit superior convergence.

5.3. New mixed-mode SMS variants

Because higher modes of substructures are usually harder to obtain than lower ones, it is harder to find the higher mixed modes than to find the lower ones. However, the higher modes are usually of little value in practical engineering, and so by ignoring them the new ESM degenerates easily into a recent SMS [5]. The main difference between the two methods is that $L_E + L_c + R = N$ for the exact method, whereas $L_E + L_c + R < N$ for the approximate method.

For this recent SMS, when the lower free-interface modes $\boldsymbol{\Phi}_{El}$ are absent $L_E = 0$ and $L_c + R < N$, so that the substructure displacements of Eq. (32) become those of the Craig and Bampton method. In contrast, Eq. (31) reduces to give the substructure displacements of Hurty. Hence the Craig–Bampton and Hurty methods are both limiting cases of the new SMS. Alternatively, if the redundant constrained modes $\boldsymbol{\Phi}_{cc}$ and the lower fixed-interfacial modes $\boldsymbol{\Phi}_{bl}$ are both absent, Eq. (31) reduces to give the substructure displacements of Hou's method, which is therefore another limiting case of the new SMS.

Some earlier authors, e.g., Craig and Chang [9] and Wang et al. [10], presented synthesis methods using Rubin's representation, the exact free-interface modal synthesis technique [11,12] and the exact fixed-interface one [2]. These all involve non-linear synthesis formulas based on using only lower modes in the synthesis process. The resulting non-linear equations are then solved iteratively, and this may require considerable computer time if the required precision is high. In contrast, the new SMS proposed in Ref. [5] only uses linear whole structure dynamic equations, even though the contributions of some or all of the higher modes have been included. The fact that the new SMS not only has a simple form with linear synthesis equations, but also gives high precision and efficiency, is demonstrated by recent numerical examples [5].

5.4. Convergence characteristics of the new mixed-mode ESM and mixed-mode SMS variants

Because the new mixed method has $L_E + L_c + R = N$, the substructural displacement $\boldsymbol{X}$ of Eqs. (31) or (32) is expressed accurately in terms of some lower mixed modes. The new mixed mode ESM includes two types of finite series of lower order modes in the substructural displacement $\boldsymbol{X}$. The error caused by neglecting the higher modes can be compensated for by selecting lower order modes from the other type of finite series. Therefore, the result is always accurate. As Example 2 proves, the five different cases are all ESM and they are all able to produce the result to an accuracy of at least 19 significant figures in Table 1, except for the eighth mode.

For any substructure, the lower modes are usually easier to obtain than the higher ones, whether from test data or from numerical analysis. Because the calculation of the higher

free-interface modes $\boldsymbol{\Phi}_{Eh}$, or the higher fixed-interface modes $\boldsymbol{\Phi}_{bh}$, is very complicated, it is not easy to apply free- or fixed-interface ESM. Therefore, it is easier to find the redundant constrained modes $\boldsymbol{\Phi}_{cc}$ and the lower fixed-interface modes $\boldsymbol{\Phi}_{bl}$ than to find the higher free-interface modes $\boldsymbol{\Phi}_{Eh}$. Alternatively, it is easier to find the lower free-interface modes $\boldsymbol{\Phi}_{El}$ than to find the higher fixed-interface modes $\boldsymbol{\Phi}_{bh}$. Hence the new mixed modes method does not need to calculate the higher free-interface modes, and therefore is much simplified. This is the advantage of this new method. The criterion for selecting the substructure modes used is to select those that are the easiest to calculate.

For all of the mixed-mode SMS variants, the more they differ from the above method, i.e., the fewer the number of modes selected, the greater the inaccuracy of the result. Because the approximate methods all have $L_E + L_c + R \ll N$, the substructural displacement $\boldsymbol{X}$ of Eqs. (31) or (32) is only expressed approximately in terms of some lower mixed modes. Eqs. (31) or (32) both contain two finite series of modes and so the two important parameters are the truncation frequencies $f_{EN}(= \omega_{EN}/2\pi)$ and $f_{bN}(= \omega_{bN}/2\pi)$ of, respectively, the lower free-interface modes $\boldsymbol{\Phi}_{El}$ and the lower fixed-interface modes $\boldsymbol{\Phi}_{bl}$. When the frequency $f(= \omega/2\pi)$ of the structure is less than f_{EN} and f_{bN}, $\boldsymbol{X}$ can be represented relatively accurately by Eqs. (31) and (32). Suppose that the truncation frequencies f_{EN} and f_{bN} for all substructures are the same and that $f_{bN} \leqslant f_{EN}$. Numerical examples [5] demonstrate that: when $f \leqslant f_{bN} (\leqslant f_{EN})$ the substructural displacements $\boldsymbol{X}$ can be approximated well by Eqs. (31) or (32), so that the accuracy of the system synthesis frequencies f are very good; when $f_{bN} \leqslant f \leqslant f_{EN}$, the accuracies of the synthesis frequencies f are also good and; in contrast, for $f_{EN} < f$ the error increases rapidly as f increases.

The fact that good synthesis frequencies are found when $f \leqslant f_{bN} (\leqslant f_{EN})$ is a very important and useful result in practical engineering. In the recent SMS [4], the truncation frequencies f_{EN} and f_{bN} are determined for all substructures and then the lowest of these values are used. The number of lower free- and fixed-interface modes required is not large, being chosen to ensure that $f_{bN} \leqslant f_{EN}$ and $f \leqslant f_{EN}$. Hence, the linear synthesis equations of this recent SMS give a synthesis procedure that is very easy, reliable and computationally efficient.

7. Conclusions

There are three different forms of structure displacement representation: the usual form of Eq. (5); Eq. (16) as first presented in Ref. [2], and Eq. (31) or (32), as proposed in this paper. Hence, there are three different forms of dynamical analytical methods and three different forms of ESM (with free interfaces, fixed interfaces and using mixed modes) associated with them.

In this paper, ESM variants with fixed interfaces and free interfaces have been reviewed and are significant because the usual variants of SMS are essentially different approximations to them, involving dynamic condensation.

This paper expresses substructural displacements exactly as mixed modes consisting of linear combinations of the fixed- and free-interface modes, leading to a new ESM using mixed modes. The key point of this ESM variant is that the higher free-interface modes are expressed in terms of some lower mixed modes by means of an exact expression. This new ESM has been proved by a strict analytical derivation and demonstrated by numerical examples. It has also been demonstrated that ESM with fixed or free interfaces are its two limiting cases. Thus, ESM with

free interface, fixed interface or mixed modes form a systematic framework of ESMs which are unified by the new mixed-mode ESM.

It has been demonstrated that all variants of SMS are essentially different approximations to these ESM variants. This makes the unifying function of the new mixed-mode ESM particularly important, e.g., it relates together the assumed modes-method using quasi-comparison functions and some new SMS variants, involving dynamic condensation. The new mixed-mode ESM may also make possible the development of new SMS methods and hence give new insights. For example, a recent mixed-mode SMS [6] is limited to the methods of Craig and Bampton and of Hurty when the lower free-interface modes $\boldsymbol{\Phi}_{El}$ are absent and to Hou's method when instead the redundant constrained modes $\boldsymbol{\Phi}_{cc}$ and the lower fixed-interfacial modes $\boldsymbol{\Phi}_{bl}$ are both absent.

Acknowledgements

The authors are grateful for support from the National Natural Science Foundation of China, from the Cardiff Advanced Chinese Engineering Centre of the Cardiff School of Engineering and from the UK EPSRC grant GR/RO5406/01. Thanks are also due to Professor J.H. Lin for useful discussions and help. The second author holds a chair at Cardiff University to which he will return upon completion of his appointment at City University of Hong Kong.

References

[1] W.C. Hurty, Vibration of structural systems by component mode synthesis, Journal of Engineering Mechancis Division ASCE 86 (1960) 51–59.
[2] J.B. Qiu, Z.G. Ying, F.W. Williams, Exact modal synthesis techniques using residual constraint modes, International Journal for Numerical Methods in Engineering 40 (1997) 2475–2492.
[3] L. Meirovitch, M.K. Kwak, Convergence of the classical Rayleigh–Ritz method and finite element method, American Institute of Aeronautics and Astronautics Journal 28 (1990) 1509–1516.
[4] L. Meirovitch, M.K. Kwak, Rayleigh–Ritz based substructure synthesis for flexible multibody systems, American Institute of Aeronautics and Astronautics Journal 29 (1991) 1709–1719.
[5] Ji-Bao Qiu, Zu-Guang, Ying, L.H. Yang, New modal synthesis technique using mixed modes, American Institute of Aeronautics and Astronautics Journal 35 (1997) 1869–1875.
[6] S.N. Hou, Review of modal synthesis techniques and a new approach, Shock and Vibration Bulletin 40 (4) (1969) 25–39.
[7] R.H. MacNeal, Ahybrid method of component mode synthesis, Computers & Structures 1 (1971) 581–601.
[8] S. Rubin, Improved component-mode representation for structural dynamic analysis, American Institute of Aeronautics and Astronautics Journal 13 (1975) 995–1006.
[9] R.R. Craig, C.J. Chang, Free-interface methods of substructure coupling for dynamic analysis, American Institute of Aeronautics and Astronautics Journal 14 (1976) 1633–1635.
[10] W.L. Wang, Z.R. Du, K.Y. Chen, Acta Brief commentary for modal synthesis techniques and a new improvement, Aeronautica et Astronautica Sinica 3 (1979) 32–51 (In Chinese).
[11] J.B. Qiu, Z.Y. Tan, Residual modes substructure synthesis techniques, in: Z.C. Zheng (Ed.), Proceedings of the International Conference on Vibration Engineering, Beijing, P.R. China, 1994, pp. 51–56.
[12] Z.G. Ying, J.B. Qiu, Z.Y. Tan, Exact residual modes and their synthesis techniques, Journal of Vibration Engineering 9 (1996) 38–46.
[13] R.R. Craig, M.C.C. Bampton, Coupling of substructures for dynamic analysis, American Institute of Aeronautics and Astronautics Journal 6 (1968) 1313–1319.